**Proceedings of the 9ICEG**
9th International Congress on Environmental Geotechnics
25-28 June, 2023 | Chania, Greece

https://doi.org/10.53243/ICEG2023-55

# Absorption behavior of BTEX on pyrophyllite surface based on molecular simulation

Zhixin Chen[1], and Liming Hu[1]

[1]*State Key Laboratory of Hydro-Science and Engineering,*

*Department of Hydraulic Engineering, Tsinghua University, Beijing, China*

## ABSTRACT

Benzene, toluene, ethylbenzene, and xylene (BTEX) ubiquitously exist in the contaminated subsurface, posing a potential threat to human health due to their carcinogenicity. Adsorption is a dominant factor in the environmental behavior of BTEX vapor in the soil. However, the macroscopic study based on sorption equilibrium experiments is not sufficient to provide information on the adsorption mechanism at a microscopic level. In this study, molecular simulations based on Grand Canonical Monte Carlo (GCMC) were applied to investigate the BTEX adsorption mechanism on pyrophyllite surfaces. Interaction energy and density distribution of the BTEX molecules were statistically obtained. Results showed that pyrophyllite surfaces were hydrophobic, validating our computational method. The order of adsorption capacity was m-xylene > ethylbenzene > toluene > benzene when the BTEX relative pressure ($P/P_0$) was less than 0.01 and reversed at relatively high $P/P_0$. The interaction between BTEX and pyrophyllite surface was primarily van der Waals interaction, and the order of the interaction energy was m-xylene > ethylbenzene > toluene > benzene in the first adsorption layer. The local density distribution of benzene demonstrated that benzene molecules formed multi-layer adsorption on the pyrophyllite surface at $P/P_0$ values greater than 0.05. The adsorption of the BTEX on pyrophyllite mainly depended on the interaction between BTEX molecules, as well as the pyrophyllite surface and the intermolecular interaction among absorbates. Overall, the knowledge of BTEX absorption mechanisms on pyrophyllite surfaces at the molecular scale is critical to understanding and predicting the environmental fate of BTEX in soils.

*Keywords: BTEX; Pyrophyllite; GCMC; Adsorption.*

## 1 INTRODUCTION

The presence of benzene, toluene, ethylbenzene, and xylene (BTEX) in the subsurface soil and groundwater is a great environmental concern due to their carcinogenic and mutagenic effects. These pollutants are frequently discharged from many kinds of industrial activities, posing a risk to human health. (Yu et al., 2022). BTEX compounds possess relatively high mobility, leading to their migration through the vadose zone and into the occupied building in the vapor phase at the contaminated sites, which is commonly referred vapor intrusion (DeVaull 2007). Clay minerals exhibit strong interaction with the vaporous BTEX during their migration, resulting in the formation of the adsorbed phase, which has a significant impact on the vapor intrusion process and limits the remediation efficiency. Therefore, it is of great significance to comprehend the mechanism of soil-air equilibrium of BTEX on clay mineral surfaces to enhance the ability to predict their mobility and retention of them in soils.

The high specific surface area and micropore structure of clay minerals make them favorable for the adsorption of BTEX compounds (Unger et al., 1996; Wu et al., 2022). Among various kinds of clay minerals present in soils, pyrophyllite is a typical 2:1 clay mineral with a hydrophobic (0 0 1) surface due to the electrical neutrality of the stoichiometric TOT (T: tetrahedral sheets; O: octahedral sheets) layer (Ulian et al., 2021). The TOT layers are held together along the stacking direction only by weak van der Waals interaction. With abundant distribution in soil and reactive surface property, pyrophyllite plays a crucial role in the adsorption of volatile organic compounds (VOCs) in the vapor phase. Therefore, it is necessary to focus on the adsorption behavior of BTEX in the vapor phase on the pyrophyllite surface.

Studies have been performed to investigate the adsorption behavior of BTEX on clay minerals by macroscopic batch adsorption experiments, with the majority of results suggesting that the sorption of BTEX on clay is mainly physical adsorption (Li et al., 2020). Although previous study based on macroscopic vapor adsorption experiments can obtain the adsorption isotherms, which are significant for determining the parameter values of the theoretical model, it is unable to reveal the mechanistic understanding of this adsorption behavior at the microscopic level. Molecular simulation, such as Grand Canonical Monte Carlo (GCMC) and molecular dynamic simulation (MD), has emerged as a powerful tool for modeling the thermodynamic process of adsorption behavior, offering a way to overcome the limitations of laboratory experiments and macroscopic analysis (Chen and Hu., 2022; Chen et al., 2023). One would use molecular simulation to quantify a variety of system properties when the laws that governs the interactionsbetween the atoms or molecules in the system are provided (Ciccotti et al. 2022). With the GCMC simulation, adsorption isotherms can be achieved by equilibrating the adsorbent with gaseous adsorbate molecules at a specific chemical potential and temperature (Akkermans et al. 2013). Several studies have been conducted to reveal the adsorption mechanism of vaporous organic pollutants on the adsorbent surface such as zeolite, activated carbon, and metal–organic frameworks (González-Galán et al. 2020, Li et al. 2020, Zhao et al. 2015). Recently, this simulation method has been introduced into the study of layered silicate-based adsorbents, which are clay minerals (Malani and Ayappa 2009). Wu et al. (2022) utilized GCMC simulations to study the adsorption behavior of BTX on different kaolinite surfaces in aqueous solutions. The study showed that the adsorption capacity was higher on the silicon tetrahedral surface compared to the aluminum octahedral surface due to its weaker hydrophilicity. However, the adsorption behavior of the BTEX in the vapor phase on pyrophyllite surfaces at the microscopic level is still lacking. It is expected to fill the knowledge gap of the macroscopic isotherms and the BTEX - pyrophyllite interaction mechanism via molecular simulation.

In this study, to explore the interaction between BTEX and pyrophyllite surfaces, a series of GCMC simulations were conducted at varying relative vapor pressures of BTEX. The molecular models were validated by GCMC-calculated water isotherms, which confirmed the hydrophobic nature of the pyrophyllite surface. BTEX adsorption isotherms were determined through GCMC calculations and the adsorption behavior was analyzed through an evaluation of the interaction energy distribution and BTEX molecules density distribution. The microscopic mechanisms underlying BTEX adsorption on the exterior pyrophyllite surfaces were ultimately revealed. The present findings contributes to theoretical basis for the prediction of the environmental behavior of BTEX in soil systems..

## 2 METHOD

### 2.1 Molecular models

Pyrophyllite ($[Si_4O_8][Al_2O_2(OH)_2]$) was selected as one of the representative clay minerals for the molecular simulation. The unit cell of this mineral surface was obtained from the Surface Model Database V1.5 of the INTERFACE (Heinz et al., 2013), with which a (5×3×2) periodic repeating supercell was constructed. The absence of isomorphic substitution in both the tetrahedral silicon layer and the octahedral aluminum layer of pyrophyllite results in the absence of cations on the pyrophyllite surface. Furthermore, both the upper and lower surfaces are tetrahedral silicon surfaces so that there is no hydroxyl distributed on the pyrophyllite surfaces. The structure parameters of absorbate molecules including BTEX and water molecules were represented using all-atom models, as shown in Figure 1. To avoid the influence of the periodic boundaries and the capillary condensation of the benzene, an empty gap of 80 Å was added to the mineral surfaces.

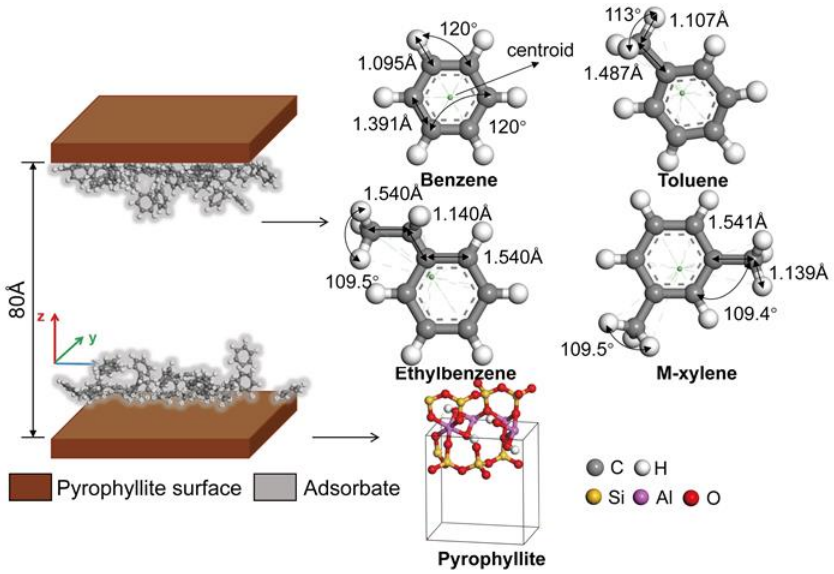


***Figure 1.*** *Schematic diagram of the GCMC models.*

## 2.2 GCMC Simulation

GCMC assumes a constant chemical potential, volume, and temperature within the system, which is the canonical ensemble. The number of BTEX molecules is allowed to fluctuate to reach the equilibrium state of the system. The simulation temperature of the system is set to 303K in this study. The chemical potential of the BTEX is associated with its pressure by the P-R equation of state.

A series of GCMC simulations were carried out by Materials Studio 2020 based on the constructed molecular models to achieve the BTEX and water adsorption isotherm on the pyrophyllite surface. The schematic diagram of the GCMC model is displayed in Figure 1. Each BTEX molecule was treated as a rigid body during the simulation. The metropolis sampling method was applied with setting exchange (39%), conformer (20%), rotate (20%), translate (20%), and regrow (2%). In this simulation, $5\times10^6$ equilibrium steps were taken to ensure that the system has reached the adsorption equilibrium state and $5\times10^6$ steps were performed for the sampling stage to obtain the average simulation results. Adsorption of BTEX on pyrophyllite surfaces was performed at a range of relative pressures ($P/P_0$) from 0.001 to 0.95. The COMPASS forcefield was selected to describe the intramolecular and intermolecular interaction of the simulated molecular system (Doi et al., 2020).

## 2.3 Data analysis

To gain a deeper understanding of the adsorption behavior of BTEX on the pyrophyllite surface at the microscopic level, the interaction energy between the adsorbates and pyrophyllite surfaces, the density distribution of BTEX molecules parallel and perpendicular to the clay surfaces were statistically calculated based on microscopic information of the simulation results. The methods of these calculations are introduced as follows.

### 2.3.1 The distribution of interaction energy between BTEX and pyrophyllite

The interaction energy between each BTEX molecule and pyrophyllite can be quantified by Equation (1), which is generally negative, implying that the BTEX molecules can be adsorbed on the pyrophyllite surface. To simplify the discussion, the absolute value of these energies was used, whereby higher values denoted more potent interactions between the clay and BTEX molecules.

$$E_{\text{inter}} = (E_{\text{BTEX}} + E_{\text{clay}}) - E_{\text{total}} \tag{1}$$

where $E_{inter}$ is the interaction energy, $E_{BTEX}$ and $E_{clay}$ represent the energy of a single BTEX molecule and the clay mineral, respectively. $E_{total}$ denotes the total energy of the system consisting of both a BTEX molecule and the clay minerals.

The distribution of the interaction energy can be obtained by the equation below:

$$f_i(E_{\text{inter}}) = \frac{\left\langle N_i\left(E_{\text{inter}} - \frac{\Delta E_{\text{inter}}}{2}, E_{\text{inter}} + \frac{\Delta E_{\text{inter}}}{2}\right)\right\rangle}{\Delta E_{\text{inter}}} \quad (2)$$

where $<N_i(E_{inter}-\Delta E_{inter}/2, E_{inter}+\Delta E_{inter}/2)>$ is the ensemble-averaged number of the adsorbate molecules within the range of $\Delta E_{inter}$ at the interaction energy value of $E_{inter}$.

2.3.2 The density distribution of BTEX on pyrophyllite surface

The pattern of the adsorbate distribution on pyrophyllite surfaces can also reflect the adsorption behaviors of BTEX molecules. To this end, the cartesian coordinates of the centroid of the adsorbates were extracted to analyze the distribution of the adsorbate parallel and perpendicular to pyrophyllite surfaces. The density distribution of the BTEX molecules normal to the pyrophyllite surface ( $\rho_i(z)$ ) can be achieved using the following equation (Deng et al., 2017) :

$$\rho_i(z) = \frac{\left\langle N_i\left(z - \frac{\Delta z}{2}, z + \frac{\Delta z}{2}\right)\right\rangle}{\Delta z} \quad (3)$$

where $<N_i(z-\Delta z/2, z+\Delta z/2)>$ is the ensemble-averaged number of the adsorbate molecules with the centroid z – axial value within the range of $\Delta z$ at the $z$ direction, and $\Delta z$ is the bin thickness. Similarly, the density distribution of the adsorbate molecules parallel to the pyrophyllite surface ( $\rho_i$ (x,y,z) ) can be obtained, which is depicted as a density field map.

## 3 Results and discussion

### 3.1 Benchmark calculation

As noted in Section 2.1, pyrophyllite surfaces lack cations or hydroxyl groups, resulting in a hydrophobic surface (Ulian et al., 2021). As a result, no water molecules will be adsorbed onto the pyrophyllite surface in the GCMC simulation if the models are constructed accurately. To validate these models, a GCMC simulation of the water isotherm on the pyrophyllite surface was conducted. The results indicated that no water molecules can be adsorbed onto the pyrophyllite surface at any relative humidity at 303 K, confirming the validity of the GCMC models. With the models validated, GCMC simulations can be performed to obtain the BTEX isotherms, establishing a connection between macroscopic experiments and microscopic phenomena.

### 3.2 BTEX isotherms

With the GCMC simulations, the average number of the adsorbed BTEX molecules $<N_w>$ at the specific $P/P_0$ was achieved. For a better description, $<N_w>$ is transferred to the concentration of the adsorbed phase $Q_s$ by the following equation:

$$Q_s = \frac{\langle N_w \rangle}{N_A \times S_m} \quad (4)$$

Where $Q_s$ is the molar mass of the adsorbed BTEX on the unit area of the mineral surface, $S_m$ is the area of the built model, and $N_A$ is the Avogadro constant.

The BTEX isotherms on pyrophyllite surfaces are shown in Figure 2. It can be seen that the order of $Q_s$ is m-xylene > ethylbenzene > toluene > benzene, when $P/P_0$ of the BTEX vapor is less than 0.01. At relatively high $P/P_0$, the order of them reversed, which is in line with the macroscopic experiments (Unger et al., 1996). This change rate of the BTEX isotherms is similar, with a sharp increase when $P/P_0$ is less than 0.1 and a slow increase thereafter. It indicates that the adsorption mechanism of these four contaminants might change after $P/P_0 = 0.1$.

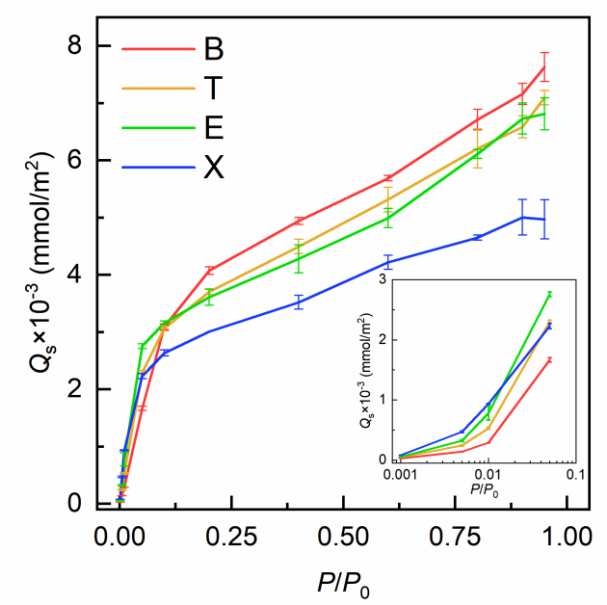


***Figure 2.*** *The adsorption isotherms of benzene (B), toluene (T), ethylbenzene (E), and m-xylene (X) on pyrophyllite surfaces at 303 K.*

### 3.3 Microscopic analysis

With the GCMC simulations, the configurations of the absorbed BTEX molecules were recorded every 1000 steps at the equilibrium state of the simulation systems. The microscopic condition of the adsorbed BTEX can be obtained by statistical analysis with these configurations, which will be discussed in the following sections.

#### 3.3.1 The interaction energy distribution

As shown in Figure 3, the total interaction energy between the pyrophyllite and BTEX molecules increases with the increase of $P/P_0$. This growth is due to the increase in the number of adsorbed molecules. It is worth noting that van der Waals interaction dominates the interaction between the pyrophyllite and BTEX molecules, while the ratio of the electrostatic interaction is ignorable. The interaction energy distributions between the BTEX molecules and pyrophyllite surface at different $P/P_0$ were calculated as mentioned in Section 2.3.1, which is shown in Figure 4. The change of patterns of interaction energy distributions from unimodal peak to bimodal peak with the increase of $P/P_0$ indicates the formation of the multi-layer BTEX adsorption on the surface of pyrophyllite, which has significant differences in the interaction energy due to varying distance to the surface. With the increase of $P/P_0$, the peak shifts to the right for all these four pollutants, which suggests that the adsorption becomes more stable. It can be seen from Figure 4 that although four contaminants have relatively similar distribution patterns of energy, the energy distribution of ethylbenzene is more scattered than the other three contaminants. This can be attributed to the existence of the ethyl group, which results in a larger kinetic diameter of the ethylbenzene. To further reveal the influence of ehyl group at molecular level, the orientations of BTEX on the mineral surfaces are displayed in Figure 5. It can be seen that the orientations of benzene, toluene, and m-xylene molecules on the surface are relatively similar and mostly parallel to the surface, while the distance and angle between ethylbenzene molecules and the surface exhibit significant variations, which explains the more scattered energy distribution of ethylbenzene on pyrophyllite surface. In indicates that the configuration of BTEX has an influence on the interaction energy distribution of BTEX on pyrophyllite surface.

For further investigation, the comparison of the interaction energy between BTEX and pyrophyllite at $P/P_0 < 0.1$ is presented in Figure 6. It is worth noting that the order of the peak value of energy is m-xylene > ethylbenzene > toluene > benzene at low $P/P_0$, which is in line with the previous study (Wu et al., 2022). This order is also in consistence with the order of $Q_s$ that mentioned in Section 3.2, indicating that the interaction between BTEX and pyrophyllite surface determines the adsorption capacity at low $P/P_0$. Therefore, more BTEX molecules will be adsorbed onto the surfaces with stronger interaction

energy at low $P/P_0$. It can be seen from Figure 6d that the peak interaction energy value of ethylbenzene is larger than that of m-xylene at $P/P_0$ =0.05, which explains the larger adsorption capacity of ethylbenzene on pyrophyllite surface than that of m-xylene at this $P/P_0$.

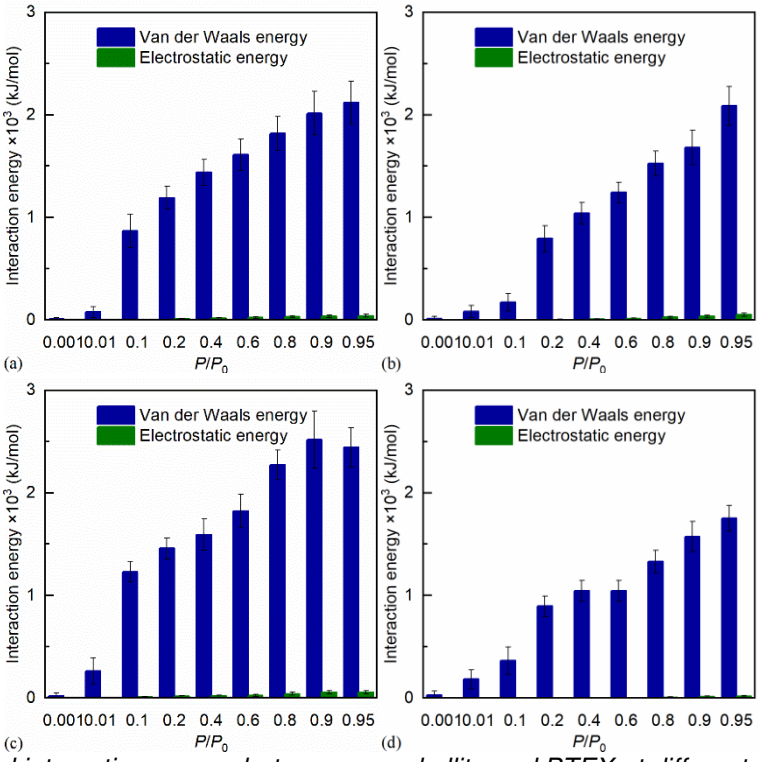


***Figure 3.*** *The total interaction energy between pyrophyllite and BTEX at different $P/P_0$. (a) benzene; (b) toluene; (c) ethylbenzene; (d) m-xylene.*

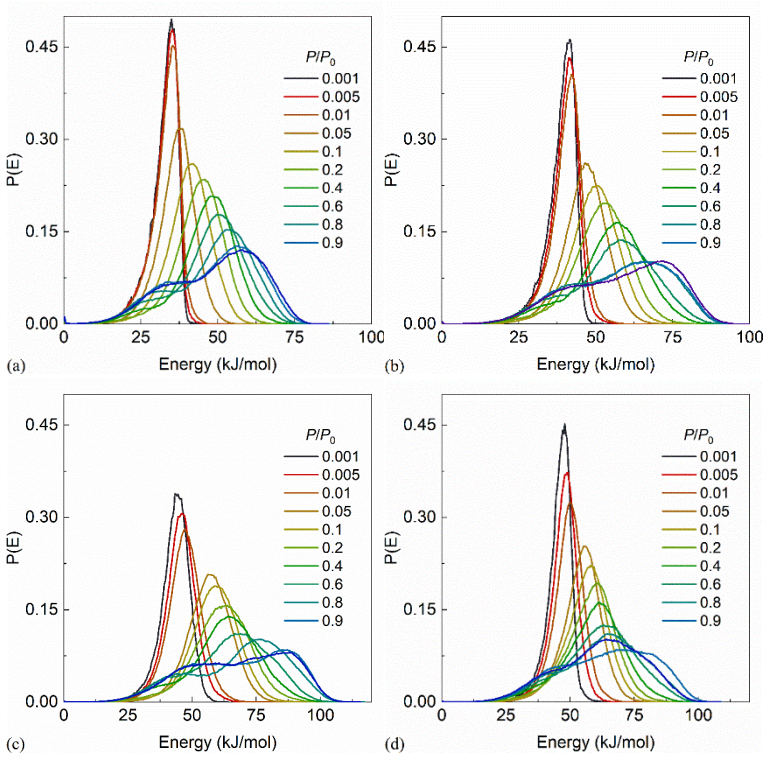


***Figure 4.*** *The distribution of interaction energy between pyrophyllite and (a) benzene; (b) toluene; (c) ethylbenzene; (d) m-xylene.*

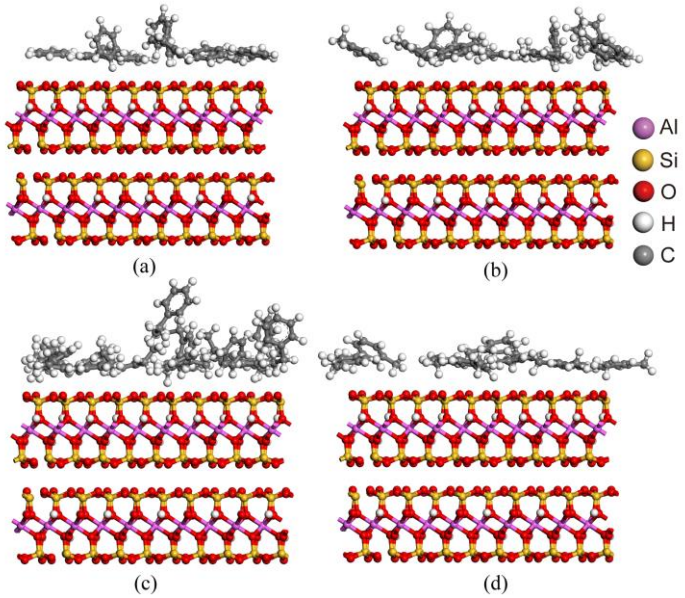


***Figure 5.*** *The configuration of BTEX molecules on pyrophyllite surfaces at $P/P_0$ = 0.05. (a) benzene; (b) toluene; (c) ethylbenzene; (d) m-xylene.*

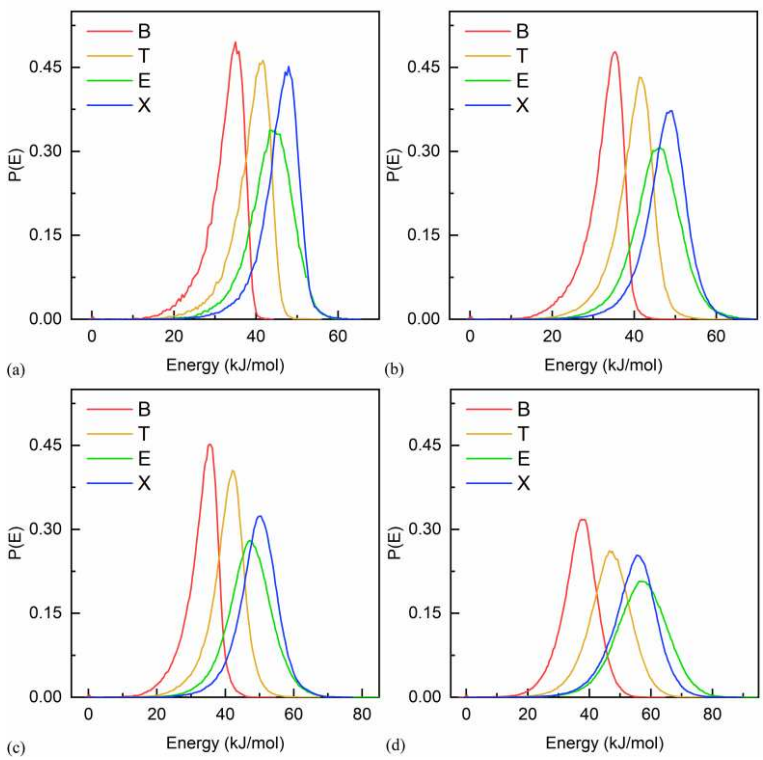


***Figure 6.*** *The distribution of intermolecular interaction energy between BTEX and pyrophyllite. (a) $P/P_0$ = 0.001; (b) $P/P_0$ = 0.005; (c) $P/P_0$ = 0.01; (d) $P/P_0$ = 0.05.*

### 3.3.2 The density distribution

As shown in Figure 7, the local density distributions (along the depth of the vaccum layer) of BTEX molecules exhibit symmetrical due to the same structure of the up and low surface of pyrophyllite. The formation of the second adsorption layer is observed when $P/P_0$ exceeds 0.1, which is consistent with the changes in the interaction energy distribution. The thickness of the first layer is estimated to be 5 Å, which is close to the thickness of the second layer. With the relatively thick first layer, the influence of the pyrophyllite surface on the adsorption of the second layer is weakened, which can be seen from the bimodal peak distribution of the interaction energy after $P/P_0$ >0.1. Due to the coverage of the

pyrophyllite surface by the first layer of BTEX molecules at high $P/P_0$, the interaction between the first and second adsorption layers will determine the adsorption of the second layer. It is shown in Figure 7 that the peak value of the second layer of m-xylene is significantly less than the other three benzene series when $P/P_0$ =0.8, indicating the smallest interaction among m-xylene molecules among the BTEX compounds.

To reflect the distribution of BTEX molecules along the pyrophyllite surface, the density field maps of the BTEX molecules were obtained by statistically analyzing the snapshots of the absorbed BTEX at $P/P_0$ = 0.05, where only one layer of BTEX molecules was absorbed onto the surface. There are three kinds of adsorption sites on the pyrophyllite surface, including the hollow site, bridge site, and top site (Wu et al., 2022), as shown in Figure 8. The calculation of density field maps reveals the preferential adsorption sites for BTEX molecules by the comparison of the density value at different sites, which contributes to revealing the adsorption mechanism of the BTEX adsorption on the pyrophyllite surface. As depicted in Figure 8, the order of BTEX density on the surface is m-xylene > ethylbenzene > toluene > benzene, which is consistent with the macroscopic isotherms shown in Figure 2. It can be seen from Figure 8 that the adsorption sites of benzene on the surface tend to be adsorbed at the hollow sites, whereas toluene prefers to be adsorbed on top sites. Ethylbenzene demonstrates a preference for both top and bridge sites, and m-xylene shows a preference for both hollow and top sites.

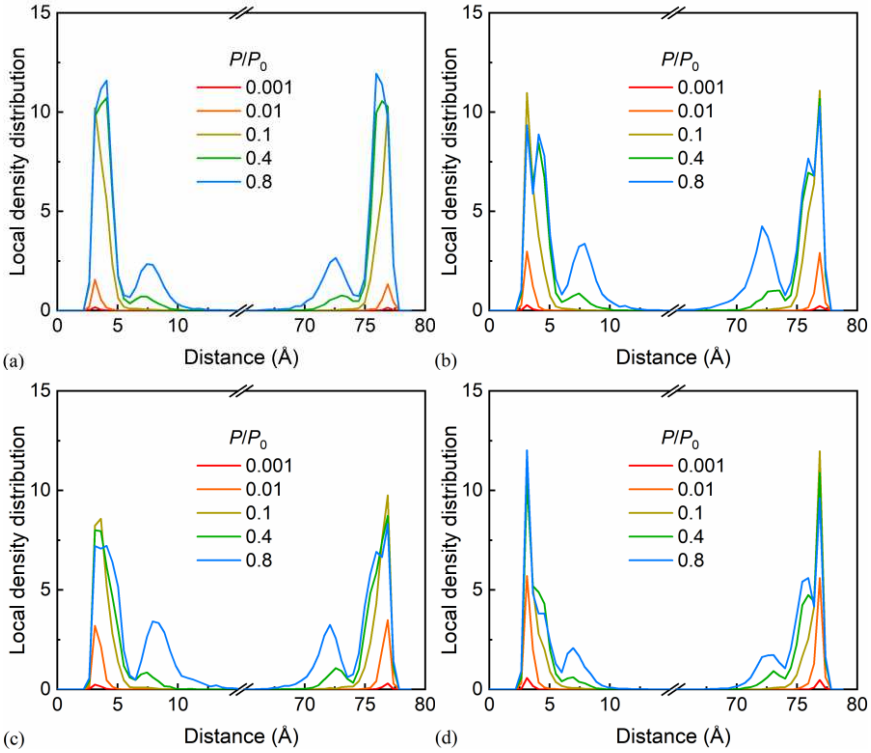


***Figure 7.*** *The local density distributions of BTEX molecules on the pyrophyllite surface. (a) benzene; (b) toluene; (c) ethylbenzene; (d) m-xylene.*

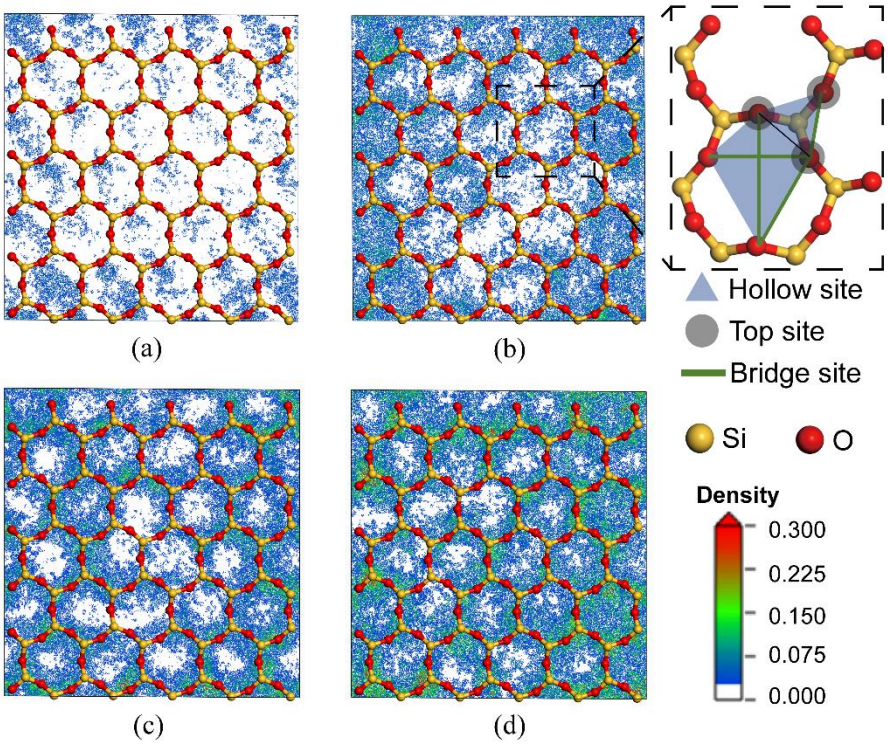


***Figure 8.*** *The density maps of BTEX molecules on the pyrophyllite surface at = $P/P_0$ 0.05. (a) benzene; (b) toluene; (c) ethylbenzene; (d) m-xylene.*

## 4 CONCLUSIONS

In this study, a series of GCMC simulations were performed to investigate the adsorption behavior of BTEX on the pyrophyllite surface. Different adsorption behavior of BTEX molecules on the surface was investigated by means of statistical analysis. The key findings are shown as follows:
(1) The adsorption of the vaporous BTEX to the clay mineral surface evolves from single layer to double layers as the increase of relative vapor pressure, indicating that both the interaction between BTEX and pyrophyllite surface and interaction among the BTEX molecules determine the macroscopic isotherms curves, which are mainly van der Waals interaction.
(2) At low $P/P_0$ before the beginning of the second adsorption layer, the interaction energy between the BTEX and pyrophyllite surface controls the adsorption capacity of the first adsorption layer, while the interaction among BTEX molecules determines the adsorption capacity of the second layer.
(3) With the existence of the methyl and ethyl, the polarity of the benzene molecules changes, inducing different configurations and preferable adsorption sites for the BTEX to be adsorbed onto, which influences the macroscopic BTEX isotherms.

## 5 ACKNOWLEDGEMENTS

This work was supported by the National Key Research and Development Program of China (2020YFC1806502) and the National Natural Science Foundation of China (51979144). The molecular simulation in this study was supported by the Center of High-Performance Computing, Tsinghua University.

## REFERENCES

Akkermans R. L. C., Spenley N. A., Robertson S. H., (2013). Monte Carlo methods in Materials Studio. Molecular Simulation, 39(14-15): 1153-1164.

Chen Z, Hu L. (2022). Adsorption of Naphthalene on Clay Minerals: A Molecular Dynamics Simulation Study. Materials, 15(15): 5120.

Chen Z., Wang Y., Hu L. (2023). Thermal desorption mechanism of n-dodecane on unsaturated clay: Experimental study and molecular dynamics simulation. Environmental Pollution, 323: 121228.

Ciccotti G., Dellago C., Ferrario M., et al., 2022, Molecular simulations: past, present, and future (a Topical Issue in EPJB). The European Physical Journal B, 95(1).

Deng L., Yuan P., Liu D., et al., (2017). Effects of microstructure of clay minerals, montmorillonite, kaolinite and halloysite, on their benzene adsorption behaviors. Applied Clay Science, 143: 184-191.

DeVaull G. E., (2007). Indoor vapor intrusion with oxygen-limited biodegradation for a subsurface gasoline source. Environ Sci Technol, 41(9): 3241-3248.

Doi A., Khosravi M., Ejtemaei M., et al., (2020). Specificity and affinity of multivalent ions adsorption to kaolinite surface. Applied Clay Science, 190: 105557.

González-Galán C., Luna-Triguero A., Vicent-Luna J. M., et al., (2020). Exploiting the π-bonding for the separation of benzene and cyclohexane in zeolites. Chemical Engineering Journal, 398: 125678.

Heinz H., Lin T. J., Mishra R. K., et al., (2013). Thermodynamically consistent force fields for the assembly of inorganic, organic, and biological nanostructures: the INTERFACE force field. Langmuir, 29(6): 1754-1765.

Li S., Song K., Zhao D., et al., (2020). Molecular simulation of benzene adsorption on different activated carbon under different temperatures. Microporous and Mesoporous Materials, 302: 110220.

Li Y., Wei M., Liu L., et al., (2020). Adsorption of toluene on various natural soils: Influences of soil properties, mechanisms, and model. Sci Total Environ, 740: 140104.

Malani A., Ayappa K., (2009). Adsorption isotherms of water on mica: redistribution and film growth. The Journal of Physical Chemistry B, 113(4): 1058-1067.

Ulian G., Moro D., Valdrè G., (2021). Water adsorption behaviour on (001) pyrophyllite surface from ab initio Density Functional Theory simulations. Applied Clay Science, 212: 106221.

Unger D. R., Lam T. T., Schaefer C. E., et al., (1996). Predicting the effect of moisture on vapor-phase sorption of volatile organic compounds to soils. Environmental science & technology, 30(4): 1081-1091.

Wu M., Zhao Z., Cai G., et al., (2022). Adsorption behaviour and mechanism of benzene, toluene and m-xylene (BTX) solution onto kaolinite: Experimental and molecular dynamics simulation studies. Separation and Purification Technology, 291: 120940.

Yu B., Yuan Z., Yu Z., et al., (2022). BTEX in the environment: An update on sources, fate, distribution, pretreatment, analysis, and removal techniques. Chemical Engineering Journal, 435: 134825.

Zhao Z., Wang S., Yang Y., et al., (2015). Competitive adsorption and selectivity of benzene and water vapor on the microporous metal organic frameworks (HKUST-1). Chemical Engineering Journal, 259: 79-89.